Self-Assembled Cationic Polypeptide Supramolecular Nanogels for Intracellular DNA Delivery

Sharafudheen Pottanam Chali,[a] Sabine Hüwel,[b] Andrea Rentmeister,[b] and Bart Jan Ravoo*[a]

Abstract: Supramolecular nanogels are an emerging class of polymer nanocarriers for intracellular delivery, due to their straightforward preparation, biocompatibility, and capability to spontaneously encapsulate biologically active components such as DNA. A completely biodegradable three-component cationic supramolecular nanogel was designed exploiting the multivalent host-guest interaction of cyclodextrin and adamantane attached to a polypeptide backbone. While cyclodextrin was conjugated to linear poly-L-lysine, adamantane was grafted to linear as well as star shaped poly-L-lysine. Size control of nanogels was obtained with the increase in the length of the host and guest polymer. Moreover, smaller nanogels were obtained using the star shaped polymers because of the compact nature of star polymers compared to linear polymers. Nanogels were loaded with anionic model cargoes, pyranine and carboxyfluorescein, and their enzyme responsive release was studied using protease trypsin. Confocal microscopy revealed successful transfection of mammalian HeLa cells and intracellular release of pyranine and plasmid DNA, as quantified using a luciferase assay, showing that supramolecular polypeptide nanogels have significant potential in gene therapy applications.

Introduction

Developments in the fields of polymer chemistry and nanotechnology have led to a broad variety of cell delivery vehicles, such as vesicles, micelles, core shell nanoparticles and nano containers.[1] Therapeutic and imaging agents such as drugs, proteins, peptides, RNA, and DNA, can be efficiently delivered into cells using these nano carriers.[2] Various nanoscale architectures have been developed for gene delivery in the past years with the aim to treat genetic disorders such as Parkinson's disease, cystic fibrosis, diabetes and hemophilia.[3] For the delivery of mRNA vaccines, only cationic lipid nanoparticles are known sofar.[4] Beyond "lipoplexes" of cationic lipids and "polyplexes" of cationic polymers, nanogels (NGs) and supramolecular nanoparticles (SNPs) emerged as potential candidates for gene delivery.[5] NGs are nanoparticles composed of a chemically or physically cross-linked hydrophilic polymer network, whereas SNPs are nanoparticles formed by selective non-covalent multivalent supramolecular interactions in a multicomponent system.[6] NGs were first reported using crosslinked poly(ethylene oxide) (PEO) and poly(ethyleneimine) (PEI) and were used for the delivery of small molecule drugs and oligonucleotides.[7]

Host-guest interaction between macrocylic host molecules (such as cyclodextrins (CDs), calixarenes, and cucurbiturils) and suitable guest molecules have been exploited for the design of various classes of supramolecular nanosystems, which are being used in different biomedical applications.[8] CD based host-guest systems are frequently explored for the preparation of supramolecular nanosystems because of their excellent biocompatibility, low cost, water solubility, easy modification of host and guest.[9] Our group developed supramolecular nanocontainers based on cyclodextrin vesicles (CDV), which were used for the intracellular delivery of hydrophilic and amphiphilic cargoes after the formation of poly(acrylate) or poly(peptide) shells on the CDV via CD and adamantane (Ad) host-guest complexation.[10] Tseng and coworkers reported size controllable SNPs based on CD/Ad recognition using three components, Ad-grafted polyamidoamine dendrimer (n-Ad-PAMAM), β-CD grafted polyethylenimine (CD-PEI) and Ad-terminated polyethylene glycol (Ad-PEG),[11] These SNPs were utilised for gene delivery as well as protein delivery.[12] Huskens et al. designed SNPs composed of a multicomponent system based on a linear negatively charged polymer poly(isobutyl-*alt*-maleic acid) (PiBMA) and the monovalent Ad-PEG utilising the multivalent interactions between β-CD and p-tert-butylphenyl group (TBP), these SNPs encapsulated cargoes via electrostatic interaction.[13] A dual responsive supramolecular NG was prepared using a benzimidazole grafted dextran and thiol-β-CD. Benzimidazole enables pH responsiveness, whereas the disul-

[a] S. Pottanam Chali, Prof. Dr. B. J. Ravoo
Organic Chemistry Institute and Centre for Soft Nanoscience
Westfälische Wilhelms-Universität Münster
Corrensstrasse 36, 48149 Münster (Germany)
E-mail: b.j.ravoo@uni-muenster.de

[b] S. Hüwel, Prof. Dr. A. Rentmeister
Institute of Biochemistry
Westfälische Wilhelms-Universität Münster
Corrensstrasse 36, 48149 Münster (Germany)

Supporting information for this article is available on the WWW under https://doi.org/10.1002/chem.202101924

fide formed by thiol-β-CD responds to a reductive environment.[14]

While biocompatibility is the minimum prerequisite of nanocarriers for cellular delivery, biodegradability is the most desirable quality.[15] Biocompatibility is addressed in most of the SNPs or NGs reported, but biodegradability is only realized in very few of them. Polypeptides are biodegradable polymers which can be synthesised by N-carboxyanhydride (NCA) polymerisation in a controlled manner.[16] There are few reports on polypeptide based nanosystems for gene delivery,[17] but to the best of our knowledge, there are no reports on supramolecular NGs based on polypeptides, neither for gene delivery nor for the delivery of other bioactive components.

We herein present a novel biodegradable and biocompatible, one pot, one step self-assembly of a three component supramolecular NGs purely based on a poly-L-lysin (PLL) backbone (Figure 1). Ad conjugated linear or star shaped PLL serves as a multivalent guest polymer, CD grafted linear PLL acts as a multivalent host polymer and monovalent Ad terminated PLL is the supramolecular stopper molecule or capping agent for the NG. Keeping the length of host polymer fixed, the guest polymer length and architecture (linear vs. star shaped) was varied to see the effect on size of the NGs formed. Anionic model cargoes, pyranine (PY) and carboxyfluorescein (CF), was successfully encapsulated inside the NGs and released in the presence of peptidase enzyme trypsin, which confirmed the biodegradable nature of these NGs. Confocal microscopy revealed the intracellular release of PY from the NGs and transfection of cells with plasmid DNA was quantified using a luciferase assay.

Results and Discussion

Linear and star shaped PLL were synthesized by NCA polymerization using initiators containing one and eight primary amines respectively (Scheme 1). Non-functional triethylene glycol amine (TEG-NH_2) was chosen as the initiator for the synthesis of linear PLL. Ring opening of the ε-benzyloxycarbonyl-L-lysine-N-carboxyanhydride (ZLL-NCA) monomer by TEG-NH_2 gives triethylene glycol-poly(ε-benzyloxycarbonyl-L-lysine) (TEG-$PZLL_n$), followed by deprotection of amines gives completely water soluble triethylene glycol-poly-L-lysine (TEG-PLL_n). ^{1}H NMR was used to calculate the degree of polymerization (n), comparing the initiator peak at 3.40 ppm and the monomer peak at 3.86 ppm (Figure S1). Four linear polymers were synthesized varying the monomer to initiator ratio, with n = 50, 60, 75, 90. GPC studies were done to corroborate the NMR data and showed a monomodal chromatogram with narrow dispersity (PDI) (Figure 2b). A slight increase in PDI was also observed with increase in polymer length. Table 1 shows the number average molecular weight (Mn) from ^{1}H NMR and GPC, weight average molecular weight (Mw) and PDI of the different polymers. MALDI analysis showed a mass distribution with a separation of 262 for TEG-$PZLL_n$, corresponding to the ε-benzyloxycarbonyl-L-lysine (ZLL) repeating unit and a separation of 128 for TEG-PLL_n for the L-lysine (LL) repeating unit. MALDI also confirmed the initiation of the polymerization by TEG-NH_2, for example picking a peak at m/z = 4378 from the MALDI of TEG-$PZLL_n$ (Figure S3) it can be deduced by $4378 = [(262 \times 16) + 165 + 23]$, where 262 is the repeating unit mass, 23 belongs to Na^+ and 163 from the initiator TEG-NH_2. Similarly, MALDI spectra of the deprotected polymer TEG-PLL_n showed the presence of the initiator after deprotection (Figure S3). For the synthesis of Ad terminated

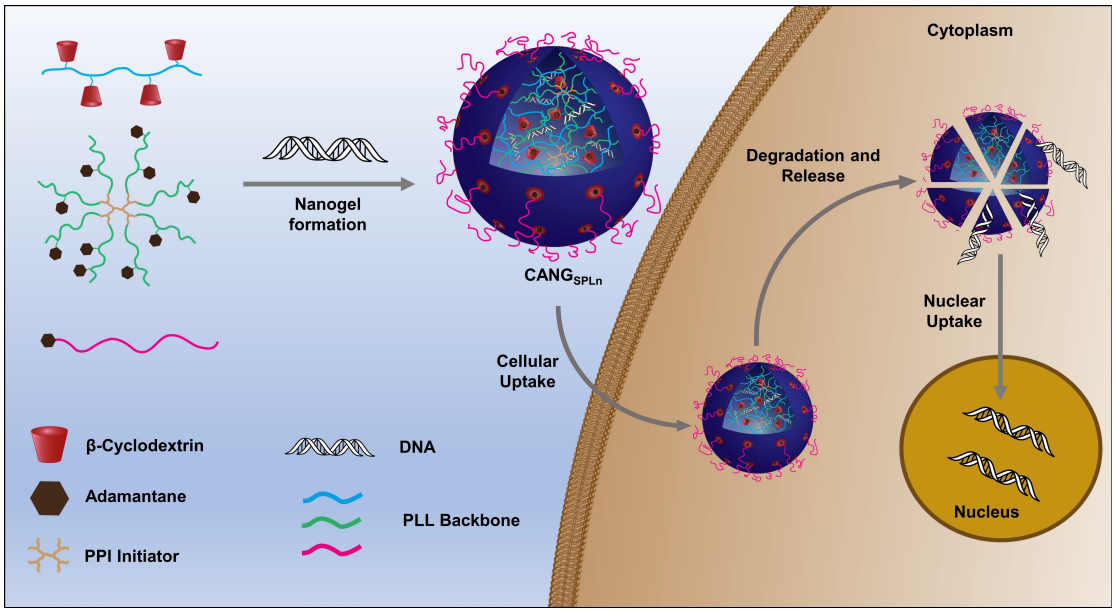

Figure 1. Design of supramolecular cyclodextrin adamantane nanogel (CANG$_{SPLn}$), from three components, 1) cyclodextrin (CD) conjugated PLL, 2) adamantane (Ad) grafted star PLL and 3) Ad terminated PLL. SPL stands for star PLL and n stands for the total number of repeating units on SPL. CANG$_{SPLn}$ was encapsulated with DNA and their cellular uptake and intracellular release is shown.

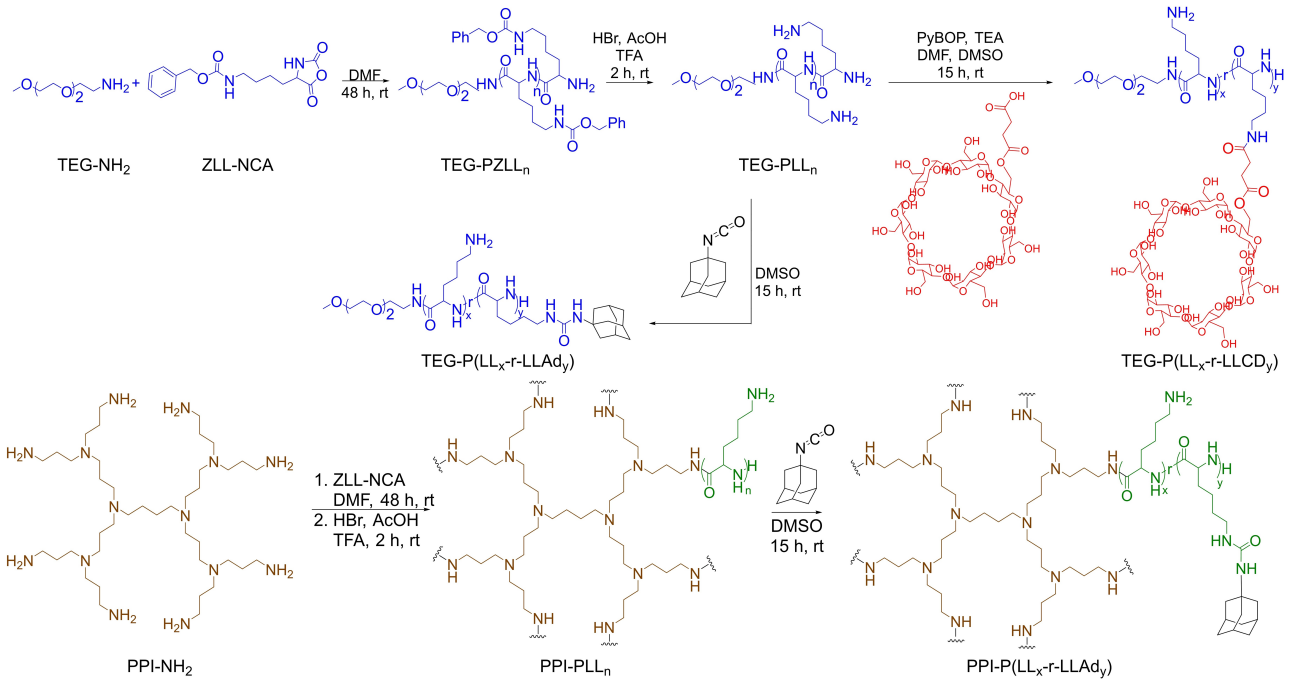

Scheme 1. Synthesis of TEG-PLL$_n$ by NCA polymerisation of ZLL-NCA monomer with initiator TEG-NH$_2$. Conjugation of Ad to TEG-PLL$_n$ using Ad isocyanate to obtain TEG-P(LL$_x$-r-LLAd$_y$) and CD to TEG-PLL$_n$ to obtain TEG-P(LL$_x$-r-LLCD$_y$). Synthesis of the star polymer PPI-PLL$_n$ using PPI-NH$_2$ initiator and grafting of Ad to obtain PPI-P(LL$_x$-r-LLAd$_y$).

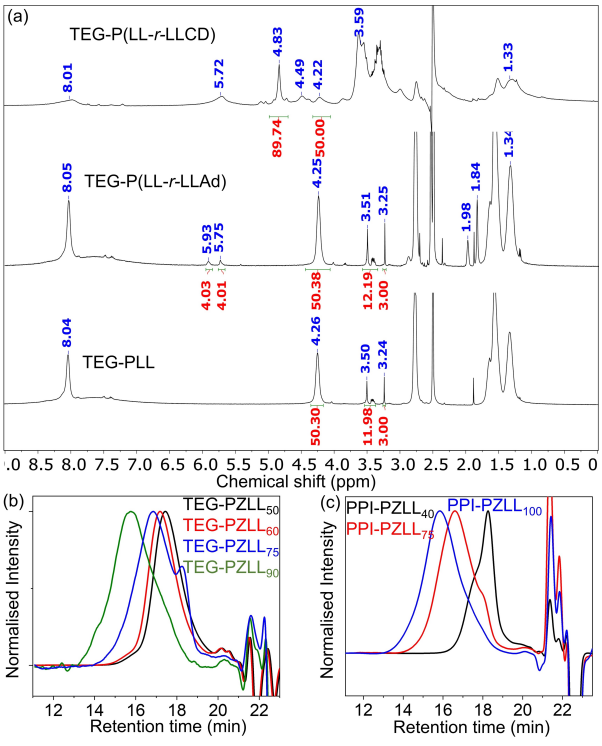

Figure 2. a) ^{1}H NMR spectra of TEG-PLL, TEG-P(LL$_x$-*r*-LLAd$_y$) and TEG-P(LL$_x$-*r*-LLCD$_y$) (DMSO-d6). Initiator peak at 3.24 ppm and repeating unit peak at 4.26 ppm was used to calculate the number of repeating units (n). For TEG-P(LL$_x$-*r*-LLAd$_y$), polymer backbone peak at 4.25 ppm and urea peak at 5.75 or 5.93 ppm formed after the conjugation of Ad is used to determine the number of Ad conjugated. The number of CD grafted was determined using the peak 4.22 ppm from the polymer backbone and 4.83 ppm from CD. GPC chromatograms of b) TEG-PZLL$_n$ and c) PPI-PZLL$_n$.

Table 1. Number of repeating units (n), number average molecular mass (M_n), weight average molecular mass (M_w) and polydispersity index (PDI) for TEG-PZLL$_n$, PPI-PZLL$_n$ and Ad-PZLL$_n$ obtained from ^{1}H NMR and GPC. n from ^{1}H NMR was calculated by comparing the initiator peak at 3.40 ppm and monomer peak at 3.86 ppm for TEG-PZLL$_n$.

Polymer	n (Aim)	^{1}H NMR		GPC			
		n	M_n [g/mol]	M_n [g/mol]	n	M_w [g/mol]	PDI
TEG-PZLL$_n$	50	50	13100	13100	50	14200	1.08
	60	61	16000	15700	60	17500	1.11
	80	77	20200	19700	75	24400	1.24
	100	88	23100	23600	90	30200	1.28
PPI-PZLL$_n$	40	–	–	11300	40	12100	1.06
	80	–	–	20300	75	23400	1.15
	110	–	–	27000	100	32900	1.22
Ad-PZLL$_n$	60	–	–	13900	52	15700	1.13

polymer, Ad methyl amine (Ad-NH$_2$) was chosen as the initiator. NCA polymerization of ZLL monomer by this initiator, followed by deprotection of the amines, gave Ad-PLL as reported in our previous publication.[10a]

Eight-armed star shaped PLL was synthesized using poly (propylene imine) dendrimer of generation 2 (PPI) as the initiator. As the PPI core has eight primary amines, the ZLL monomer is ring opened by all of these end groups and hence the eight-armed polymer is obtained. As the initiator peak overlapped with the peaks corresponding to the repeating unit, the degree of polymerization could not be deduced from ^{1}H NMR, nevertheless the broad peaks in the ^{1}H NMR indicate the formation of the polymer poly (propylene imine)-poly(ε-benzyloxycarbonyl-L-lysine) (PPI-PZLL$_n$). Instead, the degree of polymerization was determined using GPC analysis (results are

shown in Table 1). Like the linear polymers, these star shaped polymers had a monomodal chromatogram with low PDI (Figure 2c). Low PDI is usually not expected for star polymers, but this could be explained because the polymerization was done at room temperature, which would reduce the possibilities of chain terminations or other side reactions.[18] MALDI spectra of the PPI-PZLL$_n$ also showed a distribution with a separation of 262 of ZLL repeating unit. Moreover, MALDI also proved that indeed the polymer contains the PPI initiator, and it is a star polymer. Picking a peak at m/z = 6800 from the MALDI of PPI-PZLL$_n$ (Figure S4), it can be deduced by $6800 = [(262 \times 23) + 773 + 1]$, where 262 is the repeating unit mass, 1 belongs to H^+ and 773 from the initiator PPI. Deprotection of PPI-PZLL$_n$ yielded the completely water-soluble PPI-PLL$_n$. This was confirmed by ^{1}H NMR, by the disappearance of peaks at 7.22 and 4.98 ppm corresponding to the ε-benzyloxycarbonyl protecting group (Figure S2). The same was corroborated by MALDI analysis which showed a separation of 128 corresponding to the LL repeating unit (Figure S4).

As the aim of this work was the design of supramolecular NGs using a three-component system, β-CD was chosen as the host and Ad as the guest. β-CD and Ad form strong host guest complex with a binding constant, $K_a \approx 2 \times 10^4$ M^{-1}.[19] Hence, β-CD and Ad was grafted on to PLL. This study primarily focused on the effect of the guest polymer on the size and stability of the nanogels. For the synthesis of host polymer, β-CD was grafted to TEG-PLL$_{50}$. For this purpose, mono succinyl-β-CD was synthesized from β-CD using succinic anhydride. Mono succinyl-β-CD was grafted to TEG-PLL$_{50}$ by amide formation using PyBOP as a coupling reagent. The number of CD grafted on to the host polymer was determined using ^{1}H NMR (Figure 2a), and it was 12 CD for the present case. The host polymer was named triethylene glycol-poly-L-lysine-*r*-L-lysine-CD (TEG-P(LL-*r*-LLCD)).

For the synthesis of guest polymer, Ad was conjugated on to both polymers TEG-PLL$_n$ to obtain linear guest polymers and PPI-PLL$_n$ to obtain star guest polymers. Ad isocyanate was used to conjugate Ad on to the polymer backbone, as the coupling does not require any coupling reagent or harsh conditions. Moreover, the resulting urea bond with the primary amines of the polypeptides and Ad isocyanate has a specific signal in the ^{1}H NMR, which was used to quantify the number of Ad conjugated. An example is shown in Figure 2a for the case a linear polymer TEG-PLL$_{50}$, 4 Ad was conjugated, which was calculated using the urea peaks at 5.75 and 5.93 ppm. Similarly, different Ad conjugated linear and star polymers were synthesized using the TEG-PLL$_n$ and PPI-PZLL$_n$ giving triethylene glycol-poly-L-lysine-*r*-L-lysine adamantane (TEG-P(LL-*r*-LLAd)) and polypropylene imine-poly-L-lysine-*r*-L-lysine adamantane (PPI-P(LL-*r*-LLAd)). An overview of host and guest polymers TEG-P(LL$_x$-*r*-LLCD$_y$), TEG-P(LL$_x$-*r*-LLAd$_y$) and PPI-P(LL$_x$-*r*-LLAd$_y$) synthesized are listed in Table 2.

NG formation with the linear polymers was tested first. As they are formed by the host guest interaction of β-CD and Ad, these NGs were named Cyclodextrin Adamantane Nanogels (CANG$_{LPLn}$), where LPL stands for linear PLL, n is the total number of repeating units (n = x + y) of TEG-P(LL$_x$-*r*-LLAd$_y$), which is the only variable component. For the preparation of these NGs, TEG-P(LL$_x$-*r*-LLAd$_y$) and Ad-PLL$_n$ were mixed under vigorous stirring in Milli-Q water, then TEG-P(LL$_x$-*r*-LLCD$_y$) was added followed by vigorous stirring for 30 min and equilibration for 20 min. As this is a multivalent system, the importance of number and ratio of Ad and β-CD was tested. One parameter which is fixed is the guest terminated polymer Ad-PLL$_{52}$. As it bears only one Ad, Ad-PLL$_{52}$ acts as a supramolecular stopper molecule, inhibiting aggregation of particles and thus enhancing the formation of smaller particles. With the polymers having lowest number of Ad and β-CD, TEG-P(LL$_{46}$-*r*-LLAd$_4$) and TEG-P(LL$_{44}$-*r*-LLCD$_6$) no NGs were yielded with varying concentration and ratio of host to guest, which was confirmed by dynamic light scattering (DLS) measurements. This is because of the lack of host guest interaction to form a stable NG. When only the number of β-CD was increased, i.e., with TEG-P(LL$_{46}$-*r*-LLAd$_4$) and TEG-P(LL$_{38}$-*r*-LLCD$_{12}$) the result was the same, because the number of Ad was not high enough. Formation of NG was first observed with TEG-P(LL$_{38}$-*r*-LLAd$_{12}$) and TEG-P(LL$_{38}$-*r*-LLCD$_{12}$), with the third component being Ad-PLL$_{52}$. Based on the nomenclature of the NGs, this NG with components TEG-P(LL$_{38}$-*r*-LLAd$_{12}$), TEG-P(LL$_{38}$-*r*-LLCD$_{12}$) and Ad-PLL$_{52}$ is named CANG$_{LPL50}$, here 50 is the total number of repeating units of TEG-P(LL$_{38}$-*r*-LLAd$_{12}$). The concentrations of polymers were calculated based on the ratio of β-CD and Ad, i.e., the ratio of β-CD on TEG-P(LL$_{38}$-*r*-LLCD$_{12}$): Ad on TEG-P(LL$_{38}$-*r*-LLAd$_{12}$): Ad on Ad-PLL$_{52}$ is 500:450:50 μM. For this case, the size obtained was 235 nm from DLS measurements (Figure 3b,c) with a relatively narrow monomodal distribution. CANG$_{LPLn}$ were then prepared using the other three polymers TEG-P(LL$_x$-*r*-LLAd$_y$) with (x, y) = (48, 12), (61, 14), (76, 14), with the same host polymer TEG-P(LL$_{38}$-*r*-LLCD$_{12}$). When the length of the polymer was increased, the size of the CANG$_{LPLn}$ also increased (Figure 3b). The average size obtained from DLS measurements were around 235, 270, 331, 355 nm for n = 50, 60, 75, 90. This allows the design of size controllable NGs by increasing the length of the guest polymer. The zeta potential value remained a constant value of around 50 mV for all the four CANG$_{LPLn}$.

To confirm the importance of the different components, control experiments were carried out for the case of CANG$_{LPL50}$. 1) Without guest on the polymer TEG-P(LL$_{38}$-*r*-LLAd$_{12}$). i.e., TEG-PLL$_{50}$ + TEG-P(LL$_{38}$-*r*-LLCD$_{12}$) + Ad-PLL$_{52}$, the formulation did not yield any NG, because of the lack of multivalent host-guest

Table 2. Composition (*n*, *x*, *y*) and M$_n$ (g/mol) calculated from ^{1}H NMR for host and guest polymers.

Polymer	*x*	*y*	*n* = *x* + *y*	M$_n$ [g/mol]
TEG-P(LL$_x$-*r*-LLCD$_y$)	44	6	50	13900
	38	12	50	21200
TEG-P(LL$_x$-*r*-LLAd$_y$)	46	4	50	7300
	38	12	50	8700
	48	12	60	10000
	61	14	75	12200
	76	14	90	14200
PPI-P(LL$_x$-*r*-LLAd$_y$)	30	10	40	7700
	58	17	75	13400
	80	20	100	17100

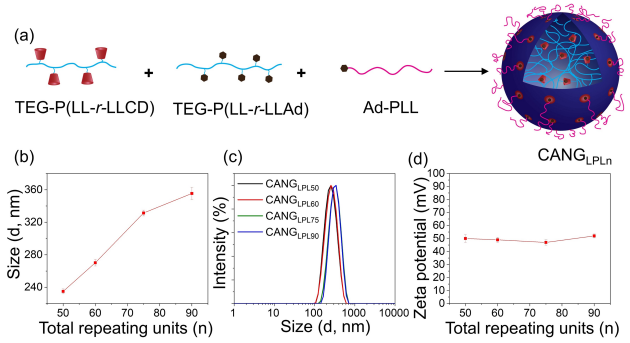

Figure 3. a) Self-assembly of CANG$_{LPLn}$ from TEG-P(LL-*r*-LLAd), TEG-P(LL-*r*-LLCD) and Ad-PLL. b) Size of CANG$_{LPLn}$ obtained from DLS measurements, total repeating units (n) is for TEG-P(LL-*r*-LLAd). c) DLS size distribution and d) Zeta potential of CANG$_{LPLn}$.

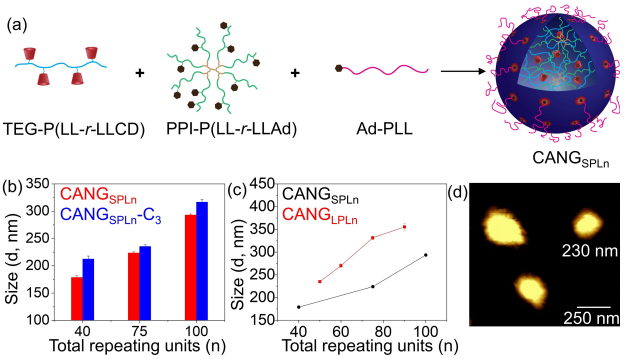

Figure 4. a) Self-assembly of CANG$_{SPLn}$ from PPI-P(LL-*r*-LLAd), TEG-P(LL-*r*-LLCD) and Ad-PLL. b) Average size of CANG$_{SPLn}$ and CANG$_{SPLn}$-C$_3$ obtained from DLS measurements, total repeating units (n) is for PPI-P(LL-*r*-LLAd). c) Average size of CANG$_{SPLn}$ and CANG$_{LPLn}$. d) AFM image of CANG$_{SPL75}$.

complexation. 2) Without host on the polymer TEG-P(LL$_{38}$-*r*-LLCD$_{12}$), i.e., TEG-P(LL$_{38}$-*r*-LLAd$_{12}$)+TEG-PLL$_{50}$+Ad-PLL$_{52}$, no NG was obtained. 3) Without Ad-PLL$_{52}$ as a stopper, NGs with a size of 248 nm (Figure S7) was formed. The size obtained in control 3 (CANG$_{LPL50}$-C$_3$) is 13 nm larger compared to the CANG$_{LPL50}$ formed with Ad-PLL$_{52}$. Ad terminated polyethylene glycol (Ad-PEG) is the only stopper molecule reported in previous reports.[20] When Ad-PEG$_{114}$ was tested to prepare CANG$_{LPL50}$, NG with similar size of 238 nm was obtained (Figure S8). These observations indicate that Ad-PLL$_{52}$ served the intended purpose as a stopper molecule. We note that all NGs discussed above were prepared in milli-Q water, and the linear guest polymer TEG-P(LL$_x$-*r*-LLAd$_y$) formed stable NGs for months in milli-Q water. However, when they were prepared in PBS buffer, the NGs aggregate within 1 min and formed a cloudy solution.

To solve the problem of aggregation and formation of unstable NGs in PBS, the linear polymer TEG-P(LL$_x$-*r*-LLAd$_y$) was replaced with the star shaped polymers PPI-P(LL$_x$-*r*-LLAd$_y$), keeping the other two components TEG-P(LL$_{38}$-*r*-LLCD$_{12}$) and Ad-PLL$_{52}$ the same, as the stability of NGs in buffer solution is important for cellular uptake and transfection. CD Ad NGs (CANG$_{SPLn}$), where SPL stands for star PLL, was prepared with the three components PPI-P(LL$_{30}$-*r*-LLAd$_{10}$), TEG-P(LL$_{38}$-*r*-LLCD$_{12}$) and Ad-PLL$_{52}$ to obtain CANG$_{SPL40}$ with a size around 180 nm. Similarly, a size of 225 nm for CANG$_{SPL75}$ and 295 nm for CANG$_{SPL100}$ was obtained when the guest polymer was changed to PPI-P(LL$_{58}$-*r*-LLAd$_{17}$) and PPI-P(LL$_{80}$-*r*-LLAd$_{20}$) respectively (Figure 4). Hence the same trend which was observed for the case of linear polymers was obtained when star polymers were used, i.e., with increase in the length of the polymers the size of the NGs also increased. Moreover, the CANG$_{SPLn}$ obtained from these star polymers were smaller than the CANG$_{LPLn}$ prepared using linear polymers of corresponding degree of polymerization (Figure 4c). For example, the size of CANG$_{SPL75}$ was 225 nm, which is 105 nm smaller than the CANG$_{LPL75}$ (size = 330 nm). The smaller size of CANG$_{SPLn}$ is due to the compact nature of the star polymer. The control without Ad-PLL$_{52}$ (CANG$_{SPLn}$-C$_3$) yielded larger NGs compared to CANG$_{SPLn}$ (Figure 4b), same as observed in the results of CANG$_{LPLn}$. CANG$_{SPLn}$ prepared using the stopper molecule Ad-PEG$_{114}$ yielded NGs of size 185 nm with the polymer PPI-P(LL$_{30}$-*r*-LLAd$_{10}$), similar to the size of 180 nm obtained with the stopper molecule Ad-PLL$_{52}$ (Figure S10). This result again confirms the effect of Ad-PLL$_{52}$ as the stopper molecule.

Atomic force microscopy (AFM) images were captured to visualize the morphology of the NGs. AFM images of CANG$_{SPLn}$ prepared using the three-star polymers are shown in Figure 4d and Figure S9, and they showed a soft and spherical morphology, which is typical for NGs. Slight variation in size and shape is expected because of the drop casting method and the water evaporation prior to imaging. Nevertheless, the size obtained was comparable to the DLS measurements. Also, an increase in size of the NGs was observed with increase in the length of the polymers, corroborating the results obtained from DLS studies.

To prove that the NGs are formed by host guest interaction of β-CD and Ad, a monovalent guest, Ad-NH$_2$ was added to the CANG$_{SPLn}$. This study was conducted with CANG$_{SPL40}$ and CANG$_{SPL75}$ (Figure S12). At lower concentration of Ad-NH$_2$ added, there was no change in size or stability of the NGs, indicating the strong multivalent host-guest interaction of the polymers. When the concentration of Ad-NH$_2$ was increased over 250 μM, the NGs start to disassemble, giving a multi modal distribution in DLS measurement. The concentration of CD present in CANG$_{SPLn}$ is 500 μM, i.e. the disassembly was only possible when Ad-NH$_2$ is at least half the concentration of CD present.

We note that also Ad-PLL$_{52}$ is a monovalent guest in the three component NG. However, when the concentration of Ad-PLL$_{52}$ was increased, no disassembly was observed (Figure 5a, Figure S13). In the absence of Ad-PLL$_{52}$ the size obtained was 192 nm, for the CANG$_{SPL40}$. At 50 μM of Ad-PLL$_{52}$, the size decreased to 180 nm, as observed in the control experiments shown before (CANG$_{SPL40}$-C$_3$). With further increase in the concentration of Ad-PLL$_{52}$, a slight increase in size was observed. The increase in size was lower at higher concentration of Ad-PLL$_{52}$. As opposed to the results observed for Ad-NH$_2$, no disassembly was observed for this case, even though Ad-PLL$_{52}$ is a monovalent guest. This is likely due to the higher molecular weight of Ad-PLL$_{52}$, which makes the CD cavities inside the NGs inaccessible. In a recent publication, we showed

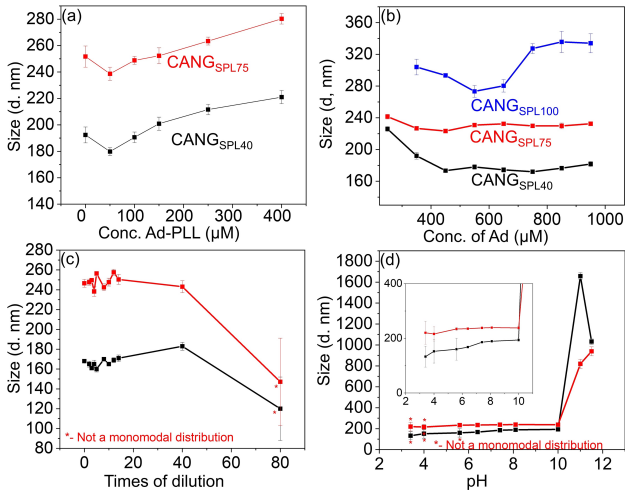

Figure 5. Average size observed with increase in the concentration of a) Ad-PLL, b) concentration of Ad on PPI-P(LL-*r*-LLAd). c) Effect of dilution on size. d) Effect of change in pH. The loss of a monomodal distribution indicates the lack of stability of NGs (Marked as red star).

that Ad terminated polypeptides such as Ad-PLL$_{52}$ are able to form host guest complex with β-CD with a binding affinity, K $\approx 5\times10^4$ M^{-1}.[10a] This finding implies that the presence of the polymer on Ad-PLL$_{52}$ does not hinder the host guest interaction of Ad and CD. The increase in size observed is because of the free CD cavities present on the surface of the NGs, which formed host guest interaction with Ad-PLL$_{52}$. This would also explain the lower increase in size at higher concentration of Ad-PLL$_{52}$, because most of the CD on the surface is already accessed by the Ad-PLL$_{52}$ added before.

In another experiment, the concentration of the guest polymer PPI-P(LL$_x$-*r*-LLAd$_y$) was changed to see the change on size, keeping the concentration of CD on TEG-P(LL$_{38}$-*r*-LLCD$_{12}$) (450 μM) and Ad-PLL$_{52}$ (50 μM) constant (Figure 5b, Figure S14). At very low concentration of Ad on PPI-P(LL$_x$-*r*-LLAd$_y$) no NG was obtained, because of the lack of host guest interaction to keep the NG stable. First stable NG was observed at 250 μM of Ad for the case of CANG$_{SPL40}$ and CANG$_{SPL75}$ and at 350 μM for the case of CANG$_{SPL100}$. With increase in concentration of Ad, a decrease and then an increase in size was observed. The larger size at lower concentration of Ad is because of the loosely connected NG. With increase in Ad containing polymer, the multivalent interaction increases, leading to the formation of more compact NGs. With further increase in the concentration, a slight increase in size was observed because the newly added guest polymer can only interact with the CDs on the surface. CANG$_{SPL100}$ is larger in size and was not stable over longer time, hence only CANG$_{SPL40}$ and CANG$_{SPL75}$ was studied in more detail.

It is important to know the stability of the NGs with dilution, because in the intended application of intracellular delivery, significant dilution is unavoidable. The two NGs CANG$_{SPL40}$ and CANG$_{SPL75}$ were subjected to dilution and the stability was analyzed using DLS measurements (Figure 5c, Figure S15). The results indicate that these NGs are at least stable up to CD and Ad concentration of 12.5 μM (40 times dilution shown in Figure 5c). Stability of the NGs in different pH is a relevant factor as there is variation from the physiological pH of 7.4 in the intracellular environment and in certain abnormal conditions such as tumors. Compared to the cytoplasmic pH of 7.4 the endosomal and lysosomal compartments have a pH around 5.5, while in the case of tumors acidic pH around 6.5 is reported.[21] Stability analysis of the NGs at different pH not only reveals their stability, but also their potential use as a pH responsive nanocarrier. CANG$_{SPL40}$ was stable in the range of pH = 6.4 to 10, whereas CANG$_{SPL75}$ was stable in the range of pH = 5.6 to 10 (Figure 5d, Figure S16). The instability at lower pH is because of the protonation of the amines present on the polymers leading to the increased electrostatic repulsion, and disintegration of the NGs. At higher pH, the solubility of the polymers is compromised, resulting in a highly turbid solution, which is also indicated by the larger size observed in the DLS measurements. Hence, the lack of stability at lower pH indicates the potential use of these NGs as pH responsive intracellular delivery vehicles.

These well characterized NGs where then loaded with dyes PY and CF as model cargo.[22] Results for the case CANG$_{SPL40}$ is shown in Figure 6 and for CANG$_{SPL75}$ is shown in Figure S17. Dyes were added along with the polymers while preparing the NGs and excess dyes were removed by dialysis. CANG$_{SPLn}$-PY indicates PY loaded NGs and CANG$_{SPLn}$-CF stands for CF loaded NGs. Figure 6a,b shows the absorbance spectra of CANG$_{SPL40}$-PY and CANG$_{SPL40}$-CF, respectively. DLS studies of these NGs showed that there was no significant change in size compared to the empty NGs even after the encapsulation of dyes (Figure 6c, Figure S17). However, zeta potential values (PBS buffer, pH = 7.4) decreased after the dye encapsulation because of the presence of negative charge on the dyes: ζ = 15 mV for empty CANG$_{SPL40}$, while ζ = 9.5 mV for CANG$_{SPL40}$-PY and ζ = 2.8 mV for CANG$_{SPL40}$-CF was observed. The larger decrease in

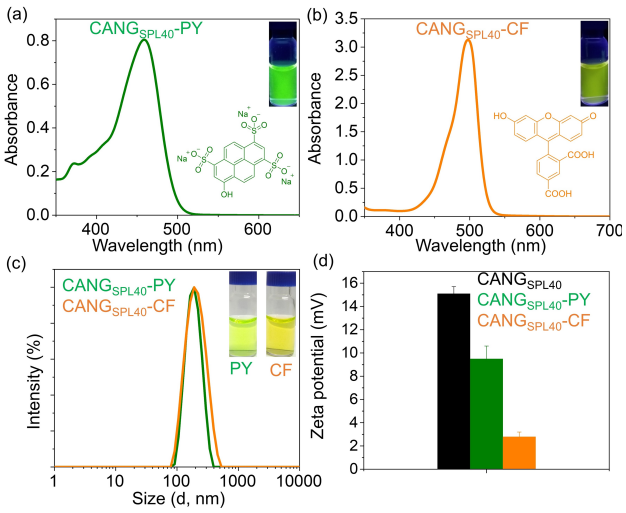

Figure 6. Absorbance spectra of a) PY encapsulated CANG$_{SPL40}$ (CANG$_{SPL40}$-PY) b) CF loaded CANG$_{SPL40}$ (CANG$_{SPL40}$-CF), inset shows the image of respective NG in a vial captured under UV light c) DLS data of CANG$_{SPL40}$-PY and CANG$_{SPL40}$-CF, inset shows their respective vial images, d) Zeta potential comparison of cargo encapsulated and empty NGs.

the case $CANG_{SPL40}$-CF was because of the higher concentration of CF present, as indicated by the absorbance measurements. Similar results were obtained for $CANG_{SPL75}$, shown in Figure S17. These results indicate the successful encapsulation of negatively charged low molecular weight cargo by these NGs.

Proteases, which are also known as peptidases, proteinases or proteolytic enzymes, are found in endosomal or lysosomal compartments.[23] Hence, cells and organisms should possess the ability to naturally degrade polypeptide NGs without releasing toxic products. To see the biodegradability and enzyme responsive release of encapsulated cargo, release studies were conducted using the two NGs loaded with PY and CF. Dye encapsulated NGs were taken in a dialysis cassette and dialysed against PBS buffer with pH = 7.4. Fluorescence of the outside solution was measured at regular intervals for 80 h. For the enzyme triggered release, trypsin was added along with the NGs in the dialysis cassette. Release from $CANG_{SPL40}$ and $CANG_{SPL75}$ was studied with two different cargoes, PY and CF, in the presence and absence of the enzyme. Fluorescence spectra obtained are normalised and are shown in Figure S18, S19. Release profiles of all the samples under the two conditions, 1) pH = 7.4 and no enzyme 2) pH = 7.4 and trypsin are shown in Figure 7. Only 14% of PY was released from $CANG_{SPL40}$ at pH = 7.4 after 80 h. But in the presence of trypsin at pH = 7.4 an enhanced release was observed. 90% of PY was released after 80 h in the presence of trypsin. This indicates the biodegradability of the PLL NGs. Similarly, only 15% of PY was released from $CANG_{SPL75}$ after 80 h. However, in the presence of trypsin the release was higher compared to $CANG_{SPL40}$. 90% PY release was already achieved after 56 h for the case of $CANG_{SPL75}$, which took 80 h in the case of $CANG_{SPL40}$. While a release of 32% was observed for $CANG_{SPL40}$ after 24 h, 50% release was observed for $CANG_{SPL75}$ in the presence of enzyme. These results showed that the release from $CANG_{SPL75}$ was faster as compared to $CANG_{SPL40}$ in the presence of trypsin. A similar release profile was observed for CF encapsulated in NGs (Figure S20).

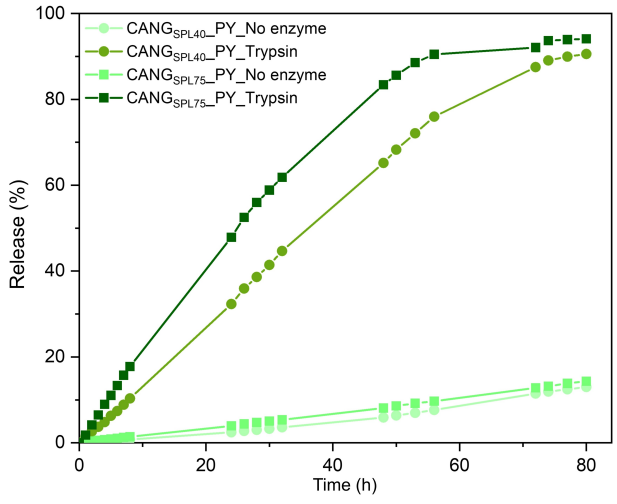

Figure 7. Release profile of PY from $CANG_{SPLn}$ in the presence and absence of enzyme trypsin at pH = 7.4. PY was encapsulated in 0.67 mg/ml $CANG_{SPLn}$.

We studied the cellular uptake of NGs using $CANG_{SPL40}$-PY and mammalian cells (Figure 8). To this end, live HeLa cells were treated with lower and higher concentration of $CANG_{SPL40}$-PY, then fixed and imaged using a confocal microscope. Cellular uptake of PY was observed for both concentrations. Cell viability studies using the MTT assay revealed that these cationic NGs are toxic at higher concentrations (Figure S21), which is common for cationic nanocarriers. Nevertheless, cells survived to confirm the transfection using these NGs leads to DNA delivery and gene expression. Importantly, the GLuc activity shown in Figure 8b is not corrected for dead cells, indicating that gene expression of the surviving cells was rather efficient. Even if there is room for improvement regarding the cell viability, formation of NGs based on dynamic host guest interactions compared to the strong electrostatic interactions in lipoplexes and polyplexes could give a significant benefit to these NGs. Moreover, the size tunability and flexible loading capacity are advantageous. Finally, we note that since proteases

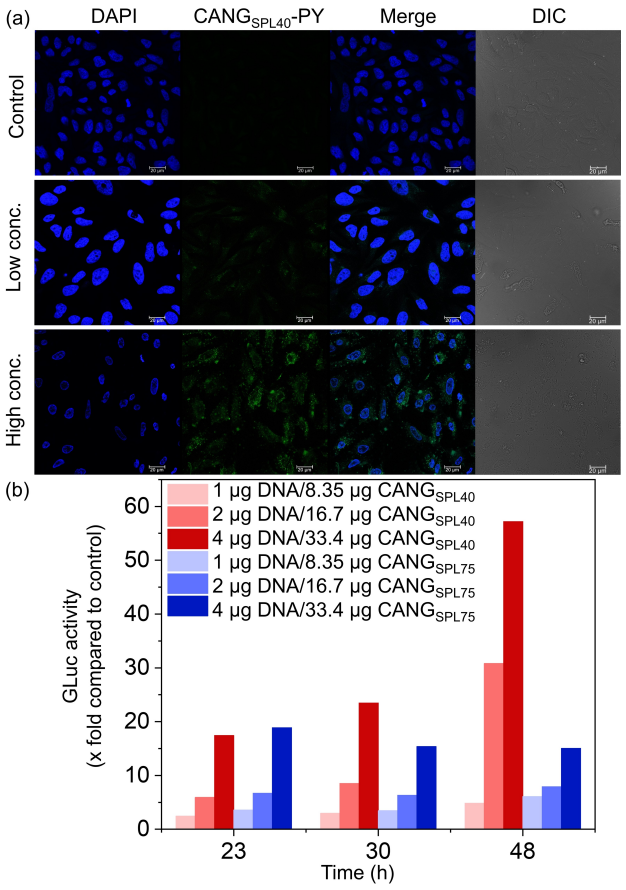

Figure 8. a) Confocal images of HeLa cells incubated with $CANG_{SPL40}$-PY and fixed using 4% paraformaldehyde (green channel represents PY; blue channel represents DAPI, which stains nuclei). Scale bar 20 µm. First row, control is without incubation of $CANG_{SPL40}$-PY. Second row, low concentration of $CANG_{SPL40}$-PY (8.35 µg $CANG_{SPL40}$, 12.5 µM PY) and third row, high concentration of $CANG_{SPL40}$-PY (33.4 µg $CANG_{SPL40}$, 50 µM PY). b) Luciferase assay results for the transfection of HeLa cells with plasmid DNA using $CANG_{SPL40}$-DNA (red bars) and $CANG_{SPL75}$-DNA (blue bars) relative to untransfected control.

are also present extracellularly, NGs not taken up by cells will be gradually degraded, reducing potential side effects.

Cationic polymers or NGs are highly explored candidates for gene delivery, because of the electrostatic interaction between negatively charged genes and positively charged polymers.[3] To test the DNA delivery capability of $CANG_{SPLn}$, plasmid DNA (GLuc_pmRNA) was encapsulated inside both NGs $CANG_{SPL40}$ and $CANG_{SPL75}$. Due to the higher electrostatic interaction between the polymers, the size obtained was smaller compared to the empty NGs (Figure S22), moreover, the zeta potential values were lower after the encapsulation of DNA. Zeta values decreased from 15 mV to 6 mV after DNA encapsulation in $CANG_{SPL40}$. To evaluate the transfection capability of these NGs, time and dose dependent transfection studies were carried out in HeLa cells. Transfection results using a luciferase assay showed that the efficiency of smaller NG $CANG_{SPL40}$ was higher as compared to $CANG_{SPL75}$ (Figure 8b). This observation is consistent with a literature report.[24] Considering that dead cells detach and do not contribute to the measured Luciferase activity, the actual transfection is efficient. Further reducing the toxicity at high concentration of CANGs can be expected to improve the overall luciferase activity and amount of protein produced.

Conclusion

The synthesis of TEG-NH_2 and Ad-NH_2 initiated linear and PPI initiated star PLL using NCA polymerization, their post polymerization modification to synthesize CD conjugated PLL as host polymer and Ad grafted guest polymer is described. Two types of NGs, $CANG_{LPLn}$ with linear Ad guest polymer and $CANG_{SPLn}$ with star Ad guest polymer were prepared, keeping the linear CD host polymer and Ad terminated polymer constant. An increase in size was observed for both the types of NGs with the increase the lengths of the Ad guest polymer. Moreover, the size obtained for $CANG_{SPLn}$ was smaller compared to $CANG_{LPLn}$ with the corresponding length of Ad guest polymer because of the compact nature of the star PLL. $CANG_{SPLn}$ were stable in PBS buffer and were able to encapsulate anionic cargoes PY, CF and DNA. Cleavage by protease and release of PY and CF was observed from $CANG_{SPLn}$. Transfection of HeLa cells and intracellular PY and DNA release was observed in HeLa cells. The latter showed that the efficiency of smaller NG, $CANG_{SPL40}$ was better compared to the larger $CANG_{SPL75}$. Hence, this novel supramolecular NG represents a potential candidate for delivery of nucleic acids for gene therapy and mRNA-based vaccination.

Acknowledgements

This work was funded by the Deutsche Forschungsgemeinschaft (DFG SFB 858) and the CIM-IMPRS Graduate School at the University of Münster. Open access funding enabled and organized by Projekt DEAL.

Conflict of Interest

The authors declare no conflict of interest.

Keywords: polypeptides · cyclodextrins · N-carboxyanhydride · ring opening polymerization · nanogels

[1] a) L. Y. T. Chou, K. Ming, W. C. W. Chan, *Chem. Soc. Rev.* **2011**, *40*, 233–245; b) D. Morshedi Rad, M. Alsadat Rad, S. Razavi Bazaz, N. Kashaninejad, D. Jin, M. Ebrahimi Warkiani, *Adv. Mater.* **2021**, *33*, 2005363; c) J. K. Patra, G. Das, L. F. Fraceto, E. V. R. Campos, M. D. P. Rodriguez-Torres, L. S. Acosta-Torres, L. A. Diaz-Torres, R. Grillo, M. K. Swamy, S. Sharma, S. Habtemariam, H.-S. Shin, *J. Nanobiotechnol.* **2018**, *16*, 71; d) S. Pottanam Chali, B. J. Ravoo, *Angew. Chem. Int. Ed.* **2020**, *59*, 2962–2972; *Angew. Chem.* **2020**, *132*, 2982–2993; e) E. Rideau, R. Dimova, P. Schwille, F. R. Wurm, K. Landfester, *Chem. Soc. Rev.* **2018**, *47*, 8572–8610; f) M. P. Stewart, A. Sharei, X. Ding, G. Sahay, R. Langer, K. F. Jensen, *Nature* **2016**, *538*, 183–192; g) T. Sun, Y. S. Zhang, B. Pang, D. C. Hyun, M. Yang, Y. Xia, *Angew. Chem. Int. Ed.* **2014**, *53*, 12320–12364; *Angew. Chem.* **2014**, *126*, 12520–12568.

[2] a) D. J. Brayden, M.-J. Alonso, *Adv. Drug Delivery Rev.* **2016**, *106*, 193–195; b) T. D. Brown, K. A. Whitehead, S. Mitragotri, *Nat. Rev. Mater.* **2020**, *5*, 127–148.

[3] a) M. A. Mintzer, E. E. Simanek, *Chem. Rev.* **2009**, *109*, 259–302; b) A. S. Piotrowski-Daspit, A. C. Kauffman, L. G. Bracaglia, W. M. Saltzman, *Adv. Drug Delivery Rev.* **2020**, *156*, 119–132; c) M. S. Shim, Y. Xia, *Angew. Chem. Int. Ed.* **2013**, *52*, 6926–6929; *Angew. Chem.* **2013**, *125*, 7064–7067; d) Y. K. Sung, S. W. Kim, *Biomaterials* **2019**, *23*, 8.

[4] a) *Nat. Nanotechnol.* **2020**, *15*, 963; b) M. D. Buschmann, M. J. Carrasco, S. Alishetty, M. Paige, M. G. Alameh, D. Weissman, *Vaccine* **2021**, *9*; c) R. A. Schwendener, *Ther. Adv. Vaccines* **2014**, *2*, 159–182.

[5] a) Q.-D. Hu, H. Fan, Y. Ping, W.-Q. Liang, G.-P. Tang, J. Li, *Chem. Commun.* **2011**, *47*, 5572–5574; b) L.-Y. Wong, B. Xia, E. Wolvetang, J. Cooper-White, *Biomacromolecules* **2018**, *19*, 353–363.

[6] a) A. V. Kabanov, S. V. Vinogradov, *Angew. Chem. Int. Ed.* **2009**, *48*, 5418–5429; *Angew. Chem.* **2009**, *121*, 5524–5536; b) S. Nayak, L. A. Lyon, *Angew. Chem. Int. Ed.* **2005**, *44*, 7686–7708; *Angew. Chem.* **2005**, *117*, 7862–7886; c) C. Stoffelen, J. Huskens, *Small* **2016**, *12*, 96–119; d) S. V. Vinogradov, T. K. Bronich, A. V. Kabanov, *Adv. Drug Delivery Rev.* **2002**, *54*, 135–147.

[7] a) S. Vinogradov, E. Batrakova, A. Kabanov, *Colloids Surf. B* **1999**, *16*, 291–304; b) T. K. Bronich, S. V. Vinogradov, A. V. Kabanov, *Nano Lett.* **2001**, *1*, 535–540.

[8] a) X. Ma, Y. Zhao, *Chem. Rev.* **2015**, *115*, 7794–7839; b) L. Wang, L. Li, Y. Fan, H. Wang, *Adv. Mater.* **2013**, *25*, 3888–3898.

[9] a) R. Mejia-Ariza, L. Graña-Suárez, W. Verboom, J. Huskens, *J. Mater. Chem. B* **2017**, *5*, 36–52; b) M. E. Davis, M. E. Brewster, *Nature Rev. Drug Dis.* **2004**, *3*, 1023–1035; c) M. E. Davis, *Mol. Pharm.* **2009**, *6*, 659–668.

[10] a) S. Pottanam Chali, B. J. Ravoo, *Macromol. Rapid Commun.* **2020**, *41*, e2000049; b) A. Samanta, M. Tesch, U. Keller, J. Klingauf, A. Studer, B. J. Ravoo, *J. Am. Chem. Soc.* **2015**, *137*, 1967–1971; c) W. C. de Vries, S. Kudruk, D. Grill, M. Niehues, A. L. L. Matos, M. Wissing, A. Studer, V. Gerke, B. J. Ravoo, *Adv. Sci.* **2019**, *6*, 1901935; d) W. C. de Vries, D. Grill, M. Tesch, A. Ricker, H. Nüsse, J. Klingauf, A. Studer, V. Gerke, B. J. Ravoo, *Angew. Chem. Int. Ed.* **2017**, *56*, 9603–9607; *Angew. Chem.* **2017**, *129*, 9732–9736.

[11] H. Wang, S. Wang, H. Su, K.-J. Chen, A. L. Armijo, W.-Y. Lin, Y. Wang, J. Sun, K. Kamei, J. Czernin, C. G. Radu, H.-R. Tseng, *Angew. Chem. Int. Ed.* **2009**, *48*, 4344–4348; *Angew. Chem.* **2009**, *121*, 4408–4412.

[12] a) Y. Liu, H. Wang, K. Kamei, M. Yan, K.-J. Chen, Q. Yuan, L. Shi, Y. Lu, H.-R. Tseng, *Angew. Chem. Int. Ed.* **2011**, *50*, 3058–3062; *Angew. Chem.* **2011**, *123*, 3114–3118; b) H. Wang, K. Liu, K.-J. Chen, Y. Lu, S. Wang, W.-Y. Lin, F. Guo, K. Kamei, Y.-C. Chen, M. Ohashi, M. Wang, M. A. Garcia, X.-Z. Zhao, C. K.-F. Shen, H.-R. Tseng, *ACS Nano* **2010**, *4*, 6235–6243.

[13] a) L. Graña-Suárez, W. Verboom, J. Huskens, *Chem. Commun.* **2014**, *50*, 7280–7282; b) L. Graña-Suárez, W. Verboom, J. Huskens, *Chem. Commun.* **2016**, *52*, 2597–2600.

[14] X. Chen, L. Chen, X. Yao, Z. Zhang, C. He, J. Zhang, X. Chen, *Chem. Commun.* **2014**, *50*, 3789–3791.

[15] a) E. Marin, M. I. Briceño, C. Caballero-George, *Int. J. Nanomed.* **2013**, *8*, 3071–3090; b) A. Mokhtarzadeh, A. Alibakhshi, H. Yaghoobi, M.

Hashemi, M. Hejazi, M. Ramezani, *Expert Opin. Biol. Ther.* **2016**, *16*, 771–785.
[16] N. Hadjichristidis, H. Iatrou, M. Pitsikalis, G. Sakellariou, *Chem. Rev.* **2009**, *109*, 5528–5578.
[17] a) Z. Song, Z. Han, S. Lv, C. Chen, L. Chen, L. Yin, J. Cheng, *Chem. Soc. Rev.* **2017**, *46*, 6570–6599; b) L. Yin, H. Tang, K. H. Kim, N. Zheng, Z. Song, N. P. Gabrielson, H. Lu, J. Cheng, *Angew. Chem. Int. Ed.* **2013**, *52*, 9182–9186; *Angew. Chem.* **2013**, *125*, 9352–9356.
[18] G. J. M. Habraken, M. Peeters, C. H. J. T. Dietz, C. E. Koning, A. Heise, *Polym. Chem.* **2010**, *1*, 514.
[19] J. Voskuhl, M. C. A. Stuart, B. J. Ravoo, *Chem. Eur. J.* **2010**, *16*, 2790–2796.
[20] C. Y. Ang, S. Y. Tan, X. Wang, Q. Zhang, M. Khan, L. Bai, S. Tamil Selvan, X. Ma, L. Zhu, K. T. Nguyen, N. S. Tan, Y. Zhao, *J. Mater. Chem. B* **2014**, *2*, 1879–1890.
[21] a) G. H. Diering, M. Numata, *Front. Plant Physiol.* **2014**, *4*, 412; b) I. F. Tannock, D. Rotin, *Cancer Res.* **1989**, *49*, 4373–4384.
[22] Johan F. G. A. Jansen, E. W. Meijer, Ellen M. M. de Brabander-van den Berg, *J. Am. Chem. Soc.* **1995**, *117*, 4417–4418.
[23] a) E. Friedmann, E. Hauben, K. Maylandt, S. Schleeger, S. Vreugde, S. F. Lichtenthaler, P.-H. Kuhn, D. Stauffer, G. Rovelli, B. Martoglio, *Nat. Cell Biol.* **2006**, *8*, 843–848; b) N. Kühnle, V. Dederer, M. K. Lemberg, *J. Cell Sci.* **2019**, *132*; c) K. Oda, *J. Biochem.* **2012**, *151*, 13–25.
[24] H. Wang, K.-J. Chen, S. Wang, M. Ohashi, K. Kamei, J. Sun, J. H. Ha, K. Liu, H.-R. Tseng, *Chem. Commun.* **2010**, *46*, 1851–1853.

Manuscript received: June 1, 2021
Accepted manuscript online: June 14, 2021
Version of record online: July 5, 2021

